

## Supporting Information

### **Assembly of Noncentrosymmetric Coordination Polymers by the Integration of Acentric Ba(II)/Sr(II) and Li(I) Coordination Polyhedra**

Ying Song,<sup>a,b</sup> Chen-Sheng Lin,<sup>a</sup> Ming-Jian Zhang,<sup>a</sup> Qi Wei,<sup>a,b</sup> Mei-Ling Feng<sup>a</sup> and Xiao-Ying Huang<sup>\*a</sup>

<sup>a</sup>State Key Laboratory of Structural Chemistry, Fujian Institute of Research on the Structure of Matter,  
Chinese Academy of Sciences, Fuzhou, Fujian 350002, P. R. China

<sup>b</sup>University of Chinese Academy of Sciences, Beijing, 100049, P. R. China

\*Corresponding author, E-mail: xyhuang@fjirsm.ac.cn Fax: (+86) 591-83793727

# 1. Experimental Section

## Materials and methods

All analytical grade chemicals employed in this study were commercially available and used without further purification. Powder X-ray diffraction (PXRD) patterns were recorded in the angular range of  $2\theta = 5-65^\circ$  on a Miniflex II diffractometer using  $\text{CuK}\alpha$  radiation. Thermogravimetric analyses were carried out with a NETZSCH STA 449F3 unit at a heating rate of  $10^\circ\text{C}/\text{min}$  under a nitrogen atmosphere. Elemental analyses (EA) for C, H, N were performed on a German Elementary Vario EL III instrument. Fourier transform infrared (FT-IR) spectra were taken on a Nicolet Magna 750 FT-IR spectrometer in the  $4000-400\text{ cm}^{-1}$  region by using KBr pellets. Optical diffuse reflectance spectra were measured at room temperature with a Varian Cary 500 Scan UV-visible system. A  $\text{BaSO}_4$  plate was used as a standard (100% reflectance). The Powder SHG (SHG) responses were measured on powdered samples by using the experimental method adapted from that reported by Kurtz and Perry.<sup>1</sup> 1064 nm radiation generated by a Q-switched Nd:YAG solid-state laser was used as the fundamental frequency light. The samples of **1** were ground and sieved into five distinct particle size ranges: 48–58, 58–75, 75–109, 109–150, and 150–212  $\mu\text{m}$ , which were pressed into a disk with diameter of 8 mm that was put between glass microscope slides and secured with tape in a 1 mm thick aluminum holder, respectively. Sieved of the standard nonlinear optical material KDP ( $\text{KH}_2\text{PO}_4$ ) samples were used as the reference in identical fashion.

## Syntheses of compounds 1-3

All the compounds were synthesized by solvothermal methods in a stainless steel reactor with a 20/28 mL Teflon liner and heated in the oven. Crystals of **1-3** were selected by hand and washed with anhydrous ethanol followed by drying in the air. The yields were calculated based on 3,5-PDCH<sub>3</sub> ligand. All the three compounds were synthesized in DMF solvent. Compound **3** can be obtained in a wide experimental conditions with temperatures between  $120^\circ\text{C}$  and  $180^\circ\text{C}$  in 3 to 8 days with or without  $\text{LiOH}\cdot\text{H}_2\text{O}$ . Sometimes **1** and **3** co-existed in one reaction while a more basic reactive environment with a larger amount of  $\text{LiOH}\cdot\text{H}_2\text{O}$  could help in obtaining the single phase of **1**. Compared to **3**, **1** could only be obtained in a relatively restrained temperature of  $150^\circ\text{C}$  in 5 days in which a gradient temperature program was needed. The structure of ligand 3,5-PDCH<sub>3</sub> is shown in Fig. S1.

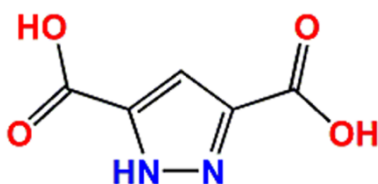


Fig. S1 Structural diagram of 3,5-PDCH<sub>3</sub> ligand utilized in this work.

**BaLi<sub>2</sub>(3,5-PDCH)<sub>2</sub>(DMF)<sub>2</sub> (1).** A mixture of 0.124 g  $\text{Ba}(\text{ClO}_4)_2$ , 0.019 g  $\text{LiNO}_3$ , 0.114 g  $3,5\text{-PDCH}_3\cdot\text{H}_2\text{O}$ , 0.013 g  $\text{LiOH}\cdot\text{H}_2\text{O}$ , and 4 mL DMF were heated by a programmed process, that is, from  $30^\circ\text{C}$  to  $150^\circ\text{C}$  within 6 hours and kept at  $150^\circ\text{C}$  for 5 days followed by being cooled to  $30^\circ\text{C}$  within 12 hours. Colorless rod-like crystals were resulted in with a yield of  $\sim 90\text{ mg}$ , 44%. Elemental analysis (%): calc. for  $\text{C}_{16}\text{H}_{18}\text{BaLi}_2\text{N}_6\text{O}_{10}$ : C, 31.73%; H, 3.00%; N, 13.88%; Found: C, 31.51%; H, 3.19%; N, 14.16%.

**SrLi<sub>2</sub>(3,5-PDCH)<sub>2</sub>(DMF)<sub>2</sub> (2).** The reaction of a mixture of 0.091 g SrCl<sub>2</sub>·2H<sub>2</sub>O, 0.036 g LiNO<sub>3</sub>, 0.113 g 3,5-PDCH<sub>3</sub>·H<sub>2</sub>O, 7 mg LiOH·H<sub>2</sub>O, and 4 mL DMF at 150 °C for 6 days resulted in colorless rod-like crystals with a yield of ~110 mg, 59%. Elemental analysis (%): calc. for C<sub>16</sub>H<sub>18</sub>Li<sub>2</sub>N<sub>6</sub>O<sub>10</sub>Sr: C, 34.57%; H, 3.26%; N, 15.12%; Found: C, 34.53%; H, 3.25%; N, 15.52%.

**[Ba<sub>3</sub>Li<sub>6</sub>(3,5-PDCH)<sub>6</sub>(DMF)<sub>2</sub>]·2DMF (3).** The reaction of a mixture of 0.087 g BaCl<sub>2</sub>·2H<sub>2</sub>O, 0.031 g LiNO<sub>3</sub>, 0.111 g 3,5-PDCH<sub>3</sub>·H<sub>2</sub>O, 6 mg LiOH·H<sub>2</sub>O, 4 mL DMF and 1 mL methanol at 120 °C for 5 days resulted in colorless rod-like crystals with a yield of ~20 mg, 10%. Elemental analysis (%): calc. for C<sub>42</sub>H<sub>40</sub>Ba<sub>3</sub>Li<sub>6</sub>N<sub>16</sub>O<sub>28</sub>: C, 30.19%; H, 2.41%; N, 13.41%; Found: C, 28.63%; H, 2.37%; N, 13.26%.

### Single-crystal structural determination

Suitable single crystals of compounds **1-3** were carefully selected under an optical microscope and glued to thin glass fibers. Data collections were performed on an Oxford Xcalibur Eos diffractometer equipped with graphite-monochromated MoK $\alpha$  radiation ( $\lambda = 0.71073$  Å) at room temperature for **1** and **2**. For compound **3**, the single-crystal diffraction data were collected on a SuperNova CCD diffractometer with graphite-monochromated MoK $\alpha$  radiation ( $\lambda = 0.71073$  Å) at 100(2) K. The structures were solved by direct methods and refined by full-matrix least-squares on  $F^2$  by using the program package SHELX-97.<sup>2</sup> All non-hydrogen atoms were refined anisotropically. The positions of hydrogen atoms were generated geometrically with assigned isotropic thermal parameters, and allowed to ride on their respective parent atoms before the final cycles of least-squares refinements. The empirical formulae were confirmed by the thermogravimetric analyses (TGA) and elemental analyses (EA) results. Details of crystallographic data and structural refinement parameters are summarized in Table S1. CCDC nos. 1036746 (**1**), 1036747 (**2**) and 1036748 (**3**) contain the supplementary crystallographic data for compounds **1-3**, respectively.

**Table S1.** Crystallographic data and structural refinement details for **1-3**.

	<b>1</b>	<b>2</b>	<b>3</b>
Empirical formula	C <sub>16</sub> H <sub>18</sub> BaLi <sub>2</sub> N <sub>6</sub> O <sub>10</sub>	C <sub>16</sub> H <sub>18</sub> Li <sub>2</sub> N <sub>6</sub> O <sub>10</sub> Sr	C <sub>42</sub> H <sub>40</sub> Ba <sub>3</sub> Li <sub>6</sub> N <sub>16</sub> O <sub>28</sub>
Formula Mass	605.58	555.86	1670.56
Crystal system	Tetragonal	Tetragonal	Orthorhombic
Space group	<i>P</i> -42 <sub>1</sub> <i>c</i>	<i>P</i> -42 <sub>1</sub> <i>c</i>	<i>P</i> 2 <sub>1</sub> 2 <sub>1</sub> 2
<i>a</i> /Å	15.0933(2)	14.7246(2)	10.8783(3)
<i>b</i> /Å	15.0933(2)	14.7246(2)	28.3945(7)
<i>c</i> /Å	10.0587(2)	10.2236(3)	9.2141(2)
<i>V</i> /Å <sup>3</sup>	2291.45(6)	2216.62(8)	2846.09(12)
<i>Z</i>	4	4	2
<i>T</i> /K	293(2)	293(2)	100(2)
Flack parameter	0.30(3)	-0.003(8)	-0.039(13)
<i>F</i> (000)	1192	1120	1628
$\rho_{\text{calcd}}$ /g cm <sup>-3</sup>	1.755	1.666	1.949
$\mu$ /mm <sup>-1</sup>	1.797	2.498	2.157
Measured refls.	6592	6272	29321

Independent refls.	2589	2432	7353
No. of parameters	165	164	433
$R_{\text{int}}$	0.0238	0.0276	0.0531
$R_1 (I > 2\sigma(I))^a$	0.0252	0.0272	0.0326
$wR(F^2) (I > 2\sigma(I))^b$	0.0470	0.0531	0.0585
GOF	1.008	1.003	1.006

$$[a] R_1 = \sum \|F_o\| - \|F_c\| / \sum \|F_o\|, [b] wR_2 = [\sum w(F_o^2 - F_c^2)^2 / \sum w(F_o^2)^2]^{1/2}.$$

### Computational Descriptions

Energy band structures and optical properties of **1** and **2** were accomplished by using the density functional theory (DFT) calculations with CASTEP code<sup>3</sup> provided by the Material Studio package. Interaction of the electrons with ion cores was represented by the norm-conserving pseudo potentials, and the valence electrons were treated as Ba, 5s<sup>2</sup>5p<sup>6</sup>6s<sup>2</sup>; O, 2s<sup>2</sup>2p<sup>4</sup>; N, 2s<sup>2</sup>2p<sup>3</sup>; C, 2s<sup>2</sup>2p<sup>2</sup>; Li, 2s<sup>1</sup>; H, 1s<sup>1</sup>. Generalized gradient approximation (GGA) in the scheme of Perdew–Burke–Eruserhof (PBE) was used to describe the exchange and correlative potential of electron–electron interactions.<sup>4</sup> The  $k$  point of first Brillouin zone was sampled as the 1×1×1 Monkhorst–Pack scheme.<sup>5</sup> Energy cutoff and precision were set to be 600 eV and 1.0×10<sup>-6</sup> eV/atom, respectively. The X-ray crystal structure data was used without further optimization. The theoretical studies of optical properties in terms of the complex dielectric function  $\varepsilon(\omega) = \varepsilon_1(\omega) + i\varepsilon_2(\omega)$  are given by

$$\varepsilon_2^{ij}(\omega) = \frac{8\pi^2 \hbar^2 e^2}{m^2 V_{\text{eff}}} \sum_k \sum_{c,v} (f_c - f_v) \frac{p_{cv}^i(k) p_{vc}^j(k)}{E_{vc}^2} \delta[E_{cv}(k) - \hbar\omega]$$

where  $\delta[E_{cv}(k) - \hbar\omega] = \delta[E_c(k) - E_v(k) - \hbar\omega]$  indicates the energy difference between the conduction and valence bands at the  $k$  point with absorption of a quantum  $\hbar\omega$ . The  $f_c$  and  $f_v$  represent the Fermi distribution functions of the conduction and valence bands, respectively. The term  $p_{cv}^i(k)$  denotes the momentum matrix element transition from the energy level  $c$  of the conduction band to the level  $v$  of the valence band at the  $k$  point in the Brillouin zones and  $V_{\text{eff}}$  is the volume of the unit cell. The  $m$ ,  $e$ , and  $\hbar$  are the electron mass, charge, and Plank's constant, respectively. Then the first-order susceptibility at low frequency region is given by  $\chi^{(1)}(\omega)_{ii} = [\varepsilon(\omega)_i - 1]/4\pi$ , and the second-order susceptibilities can be expressed in terms of the first-order susceptibilities as follows:

$$\chi_{ijk}^{(2)}(-\omega_3; \omega_1, \omega_2) = F^{(2)} \chi_{ii}^{(1)}(\omega_3) \chi_{jj}^{(1)}(\omega_1) \chi_{kk}^{(1)}(\omega_2)$$

Where  $F^{(2)} = ma/(N^2 e^3)$ . These expressions are derived from a classical anharmonic oscillator (AHO) model.<sup>6</sup> The  $m$  and  $e$  are, respectively, the electron mass and charge, and the parameter  $a$ , which characterizes the nonlinearity of the response and it is estimated as  $\omega_0^2 / d$ , where  $d$  is the lattice constant and  $\omega_0$  is the response frequency. The  $N$  is the density number of unit cell. For **1** and **2**,  $F$  is estimated to be  $5.0 \times 10^{-6}$  esu. The SHG component  $d_{ij}$  is equal to half of the corresponding  $\chi_{ij}$  value for the consequence of historical convention.

## 2. More structural details

Compounds **1-3** feature robust 3D neutral frameworks. The coordination numbers of Ba<sup>2+</sup>/Sr<sup>2+</sup> ions vary from 8 to 10 in the title structures which is similar to those for other Ba/Sr-based coordination polymers, Fig. S2.<sup>7</sup> While the Li<sup>+</sup> ion adopts a common tetrahedron coordination geometry in the three structures; and the solvent DMF molecules favorite to coordinate to Li<sup>+</sup> as terminal ligands. The Ba-O<sub>carboxylate</sub>, Ba-N, Li-O<sub>carboxylate</sub> and Li-N bond distances of the three structures all fall in the normal ranges of literature values<sup>7a, 8</sup>, that is, for **1**, Ba-O, 2.752(2) to 3.186(3) Å; Li-O, 1.848(8) to 2.391(11) Å; and **2**, Sr-O, 2.565(2) to 2.739(2) Å; Li-O, 1.857(5) to 2.214(6) Å; for **3**, Ba-O: 2.676(3) to 3.195(4) Å; Ba-N, 2.841(3) to 3.124(3) Å; Li-O, 1.899(7) and 2.043(8) Å; and Li-N, 2.140(8) Å.

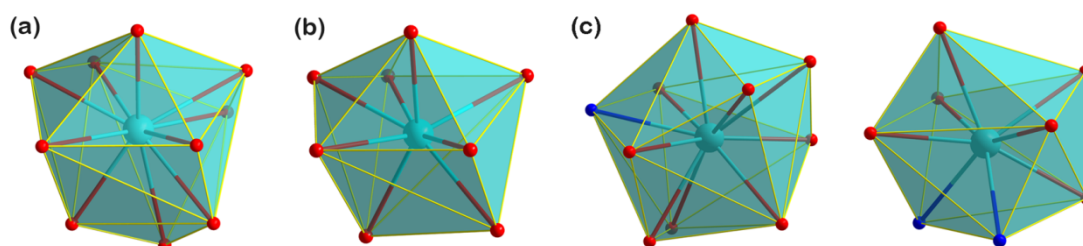


**Fig. S2** (a) The [BaO<sub>10</sub>] polyhedron in **1**; (b) the [SrO<sub>8</sub>] polyhedron in **2** and (c) the [BaO<sub>9</sub>N] and [BaO<sub>6</sub>N<sub>2</sub>] polyhedra in **3**.

The asymmetric unit of **1** contains half a formula unit including half a Ba<sup>2+</sup> ion located at the special position with 2 symmetry, one Li<sup>+</sup> ion, one 3,5-PDCH<sup>2-</sup> ligand, and one DMF molecule. The deca-coordinated Ba<sup>2+</sup> ion is occupied by eight O atoms of four symmetry related chelating carboxylate groups (O1, O2; O1, O2; O3, O4; O3, O4) and two O atoms of two symmetry related carboxylate groups (O3, O3) from six 3,5-PDCH<sup>2-</sup> ligands. The tetra-coordinated Li<sup>+</sup> center binds three carboxylate O atoms (O1, O2, O3) from three 3,5-PDCH<sup>2-</sup> ligands and one terminal DMF molecule, Fig. S3a. Thus the polyhedra around Ba<sup>2+</sup> or Li<sup>+</sup> lack an inversion center. The 3,5-PDCH<sup>2-</sup> ligand adopts a (*k*<sup>1</sup>-*k*<sup>2</sup>- $\mu_3$ )-(*k*<sup>2</sup>-*k*<sup>2</sup>- $\mu_3$ )- $\mu_6$  coordination mode, Fig. S3b.

Along the *c* axis, an infinite heterometallic [BaLi<sub>2</sub>(COO)<sub>4</sub>]<sub>n</sub> ribbon is evident in which the adjacent Ba<sup>2+</sup> ions are interlinked by two carboxylate groups ( $\mu_2$ -O3, O4,  $\mu_2$ -O3, O4) from two ligands in a double-bridging fashion, while the Li<sup>+</sup> ion binds to O3 and another two oxygen atoms (O1, O2) from two carboxylate groups that chelate to Ba<sup>2+</sup> ions, Fig. 1a. The coordinated DMF molecules are filled in the tunnels along the *c* axis, Fig. S4. The void volume of the guest-removed structure is 43.9% estimated by *PLATON* Program.

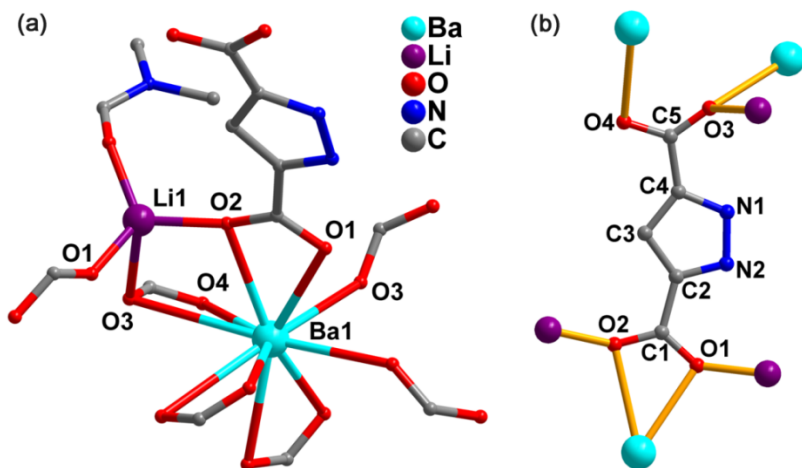


**Fig. S3** (a) The coordination modes of  $\text{Ba}^{2+}$  and  $\text{Li}^+$  ions in **1**; (b) the linking mode of  $3,5\text{-PDCH}_2^-$  ligand in **1**. All of the H atoms are omitted for clarity.

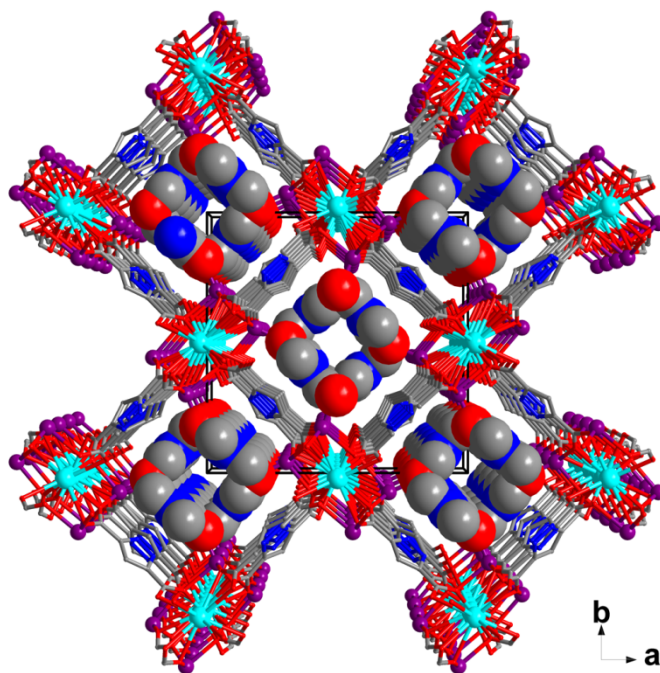


**Fig. S4** The 3D structure of **1** viewed along the  $c$  axis with coordinated DMF molecules in a space-filling mode located in the tunnels along the  $c$  axis. All of the H atoms are omitted for clarity.

In the structure of **3**, its asymmetric unit contains half of the formula unit including one and a half of  $\text{Ba}^{2+}$  ions, three  $\text{Li}^+$  ions, three  $3,5\text{-PDCH}_2^-$  ligands, one coordinated and one lattice DMF molecule. The Ba1 is deca-coordinated by two chelating carboxylate groups with four O atoms (O1, O2, O9, O10) from two  $3,5\text{-PDCH}_2^-$  ligands and one  $3,5\text{-PDCH}_2^-$  ligand with its N3 and O5 atoms, and another four O atoms from four separate  $3,5\text{-PDCH}_2^-$  ligands (O7, O10, O11, O12). While the octa-coordinated Ba2 is located at the special position with 2 symmetry, and it connects to two symmetry-related chelating ligands with four atoms (N5, O9, N5, O9) and four symmetry-related ligands with four carboxylate O atoms (O5, O8, O5, O8). The three independent  $\text{Li}^+$  ions are all tetra-coordinated. The Li1 is coordinated by one carboxylate O atom (O1), two atoms from a chelating ligand (O4

and N2) and an oxygen from a terminal DMF molecule. While the Li2 and Li3 connect to carboxylate O atoms (O4, O6, O9, O11 for Li2 and O2, O3, O5, O8 for Li3) from different 3,5-PDCH<sup>2-</sup> ligands, respectively, Fig. S5. The 3,5-PDCH<sup>2-</sup> ligands adopt three different coordination modes, i.e., (*k*<sup>1</sup>-*k*<sup>2</sup>- $\mu_3$ )-(*k*<sup>2</sup>-*k*<sup>3</sup>(O, N)- $\mu_4$ )- $\mu_7$ , (*k*<sup>1</sup>-*k*<sup>2</sup>- $\mu_3$ )-(*k*<sup>1</sup>-*k*<sup>3</sup>(O, N)- $\mu_4$ )- $\mu_7$  and (*k*<sup>1</sup>-*k*<sup>2</sup>(O, N)- $\mu_3$ )-(*k*<sup>2</sup>-*k*<sup>2</sup>- $\mu_3$ )- $\mu_6$  (denoted as L-I, L-II and L-III, Fig. S6). Note that the 3,5-PDCH<sup>2-</sup> ligands in this work link more metal ions than that in the reported structures<sup>9</sup> probably due to the small ionic radius of Li<sup>+</sup> ion.

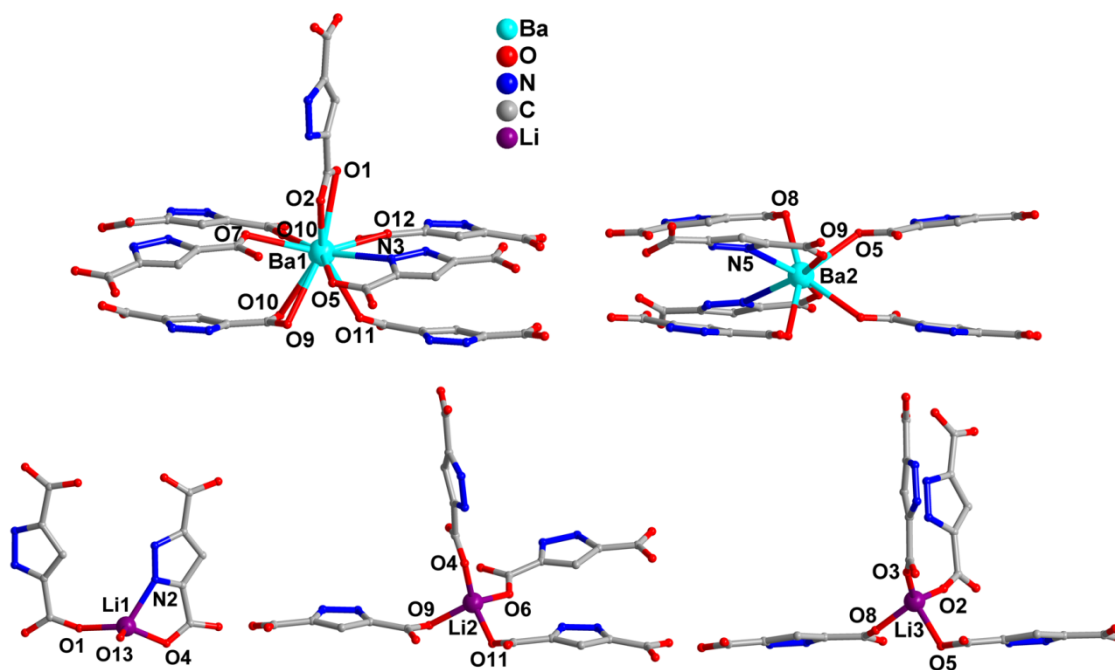


**Fig. S5** The coordination modes of metal ions Ba1, Ba2, Li1, Li2 and Li3 in **3**. All of the H atoms are omitted for clarity.

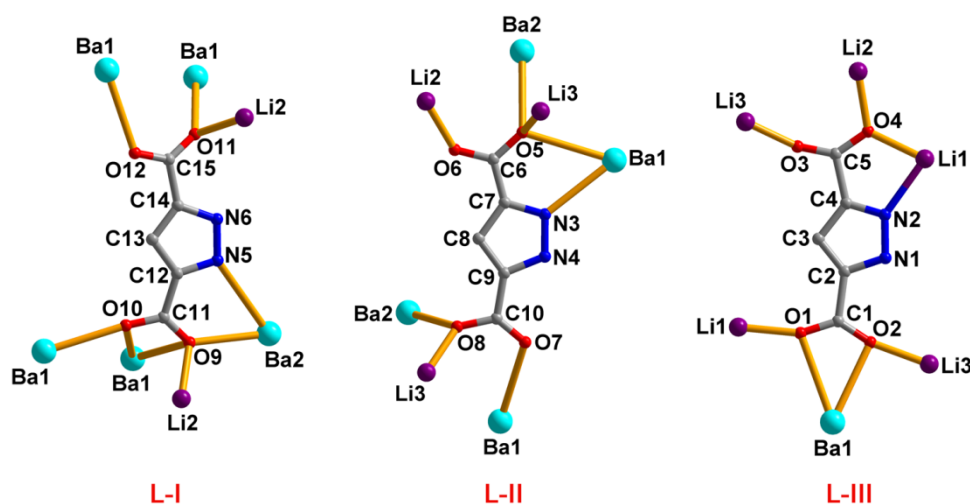


**Fig. S6** Three different coordination modes of 3,5-PDCH<sup>2-</sup> ligands in **3**. All of the H atoms are omitted for clarity.

As shown in Fig. S7, the construction of the framework of **3** could be described as follows.

Firstly, the Ba1, Ba2, Li2 and Li3 are linked by the carboxylate groups of L-I and L-II into a cluster of {Ba<sub>3</sub>Li<sub>4</sub>(COO)<sub>14</sub>}. The cluster contains one Ba2 in 2 symmetry, two Ba1, two Li2, two Li3 in both sides. The Ba1

and Ba2 are interconnected by one bridging carboxylate group (O7, O8) of L-II and two carboxylate O atoms (O5, O9) from one L-I and one L-II, which lead to an axial symmetric  $\{Ba_3\}$  unit containing one Ba2 in 2 symmetry and two Ba1 in both ends. Then, The Li3 is connected to Ba1 and Ba2 through O2 of L-III and O8 of L-II, respectively. Simultaneously, the O1 and O2 of L-III are chelated to Ba1 and  $\mu_3$ -O5 of L-II links one Li3, one Ba1 and one Ba2. The Li2 is joined to Ba1 and Ba2 through O11 of L-I and one bridging carboxylate group (O5, O6) of L-II, respectively. At the same time, the Li2, Ba1 and Ba2 are also jointed by  $\mu_3$ -O9 of L-I. One carboxylate group (O5, O6) of L-II acts as a bridge to link Li2 and Li3.

Secondly, these clusters further share carboxylate O atoms to form a 1D ribbon along the  $a$  axis, in which the linkers are two O10 of two L-I and two bridging carboxylate groups (O11 and O12) of L-I between two Ba1. Afterward the 1D ribbons are weaved by L-I and L-II into a 2D  $[Ba_3Li_4(3,5-PDCH)_4]_n$  layer parallel to the  $ac$  plane.

Finally, along the  $b$  direction, these 2D layers are interlinked by L-III as pillars to form a 3D framework (with one of its carboxylate group chelating to Ba1 and bonding to Li3 of one layer, with the other carboxylate group bonding to Li2 and Li3 in the adjacent layer). Further, Li1 links L-III into a helical chain along the  $a$  axis and the final 3D framework formed. The helical chain by Li1 linking L-III is left-handed with a pitch of 10.95 Å running along the  $2_1$ -axis parallel to the  $a$  axis.

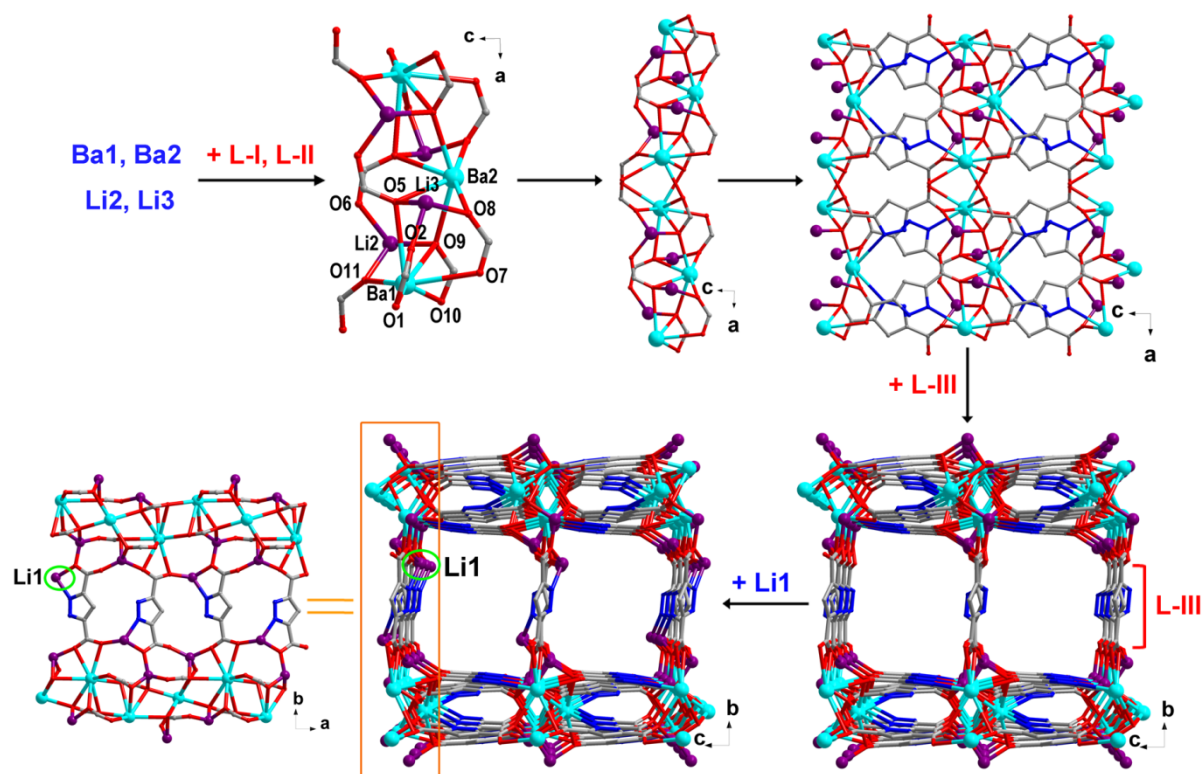


**Fig. S7** The scheme showing the construction of **3** to clearly understand its structure. All of the H atoms and DMF molecules are omitted for clarity.

Another right-handed helical chain exists by alternately linking Li2 and Ba1 by L-III and O11 of L-I with a pitch of 28.59 Å running along the  $2_1$ -axis parallel to the  $b$  axis, Fig. 2e. The free DMF molecules are found in the free spaces and all the DMF molecules are oriented towards the tunnels along the  $a$  axis, Fig. S8. The guest omitted structure has a void volume of 33% of the whole structure estimated by PLATON Program.



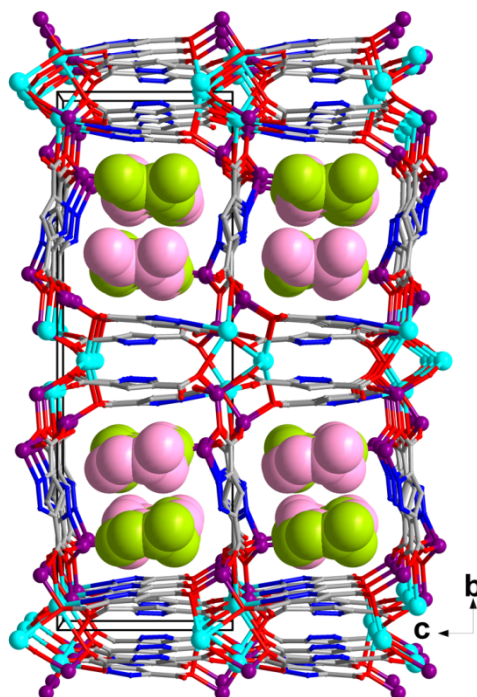


**Fig. S8** The 3D structure of **3** viewed along the *a* axis with free (rose) and coordinated (lime) DMF molecules in a space-filling mode oriented towards the tunnels parallel to the *a* axis. All of the H atoms are omitted for clarity.

### 3. PXRD Patterns

The phase purity of compounds **1-3** was confirmed by PXRD characterizations (Fig. S9) and elemental analyses.

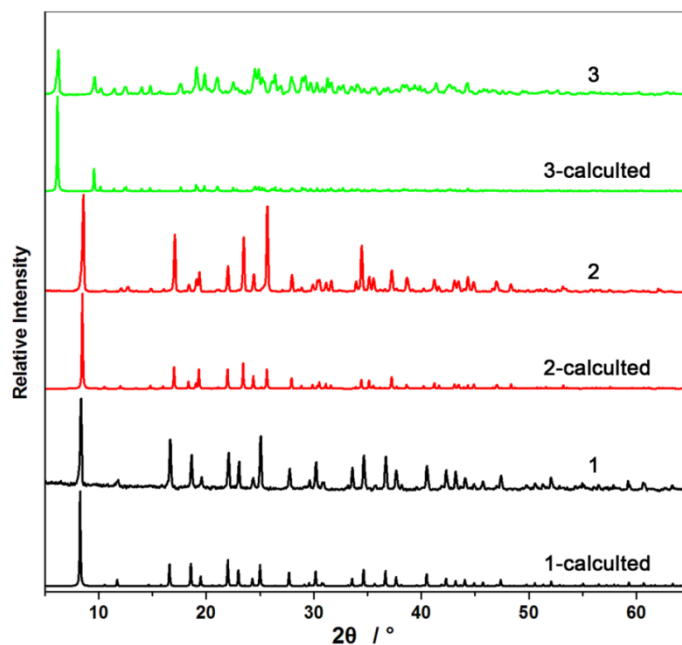


**Fig. S9** Experimental and simulated PXRD patterns of **1-3**.

## 4. Thermogravimetric Analyses

Thermogravimetric analyses (TGA) were performed on the pure powder samples of **1-3** from 30 to 800 °C, Fig. S10. **1** was stable up to 280 °C; the sharp weight loss (about 24.3%) from 280 to 355 °C corresponded to the losses of coordinated DMF molecules (calc. 24.1%) which brought about the collapse of the framework. The TGA curve of **2** has the similar tendency with that of **1**. **2** lost coordinated DMF molecules (about 25.8%, calc. 26.3%) in the temperature range of 170 to 350 °C followed by the collapse of the whole framework.

Compound **3** is not very stable when it was taken apart from the mother liquid and easily releases free DMF molecules at room temperature. In the first two steps within 350 °C, it released free and coordinated DMF molecules with a weight loss of about 14.5% which is slightly fewer than the calculated value of 17.5%, probably due to the release of a small amount of free DMF molecules (about 3%) at ambient conditions before the TGA experiment. Above 350 °C, the major framework collapsed.

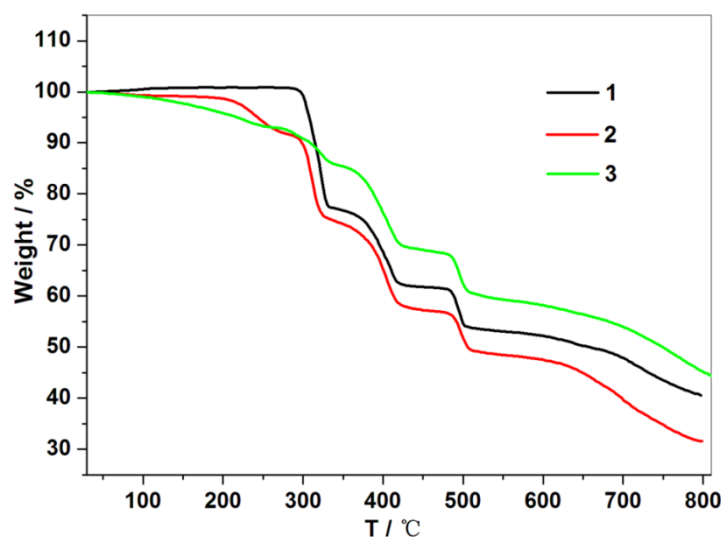


Fig. S10 TGA curves of **1-3**.

## 5. IR Spectra

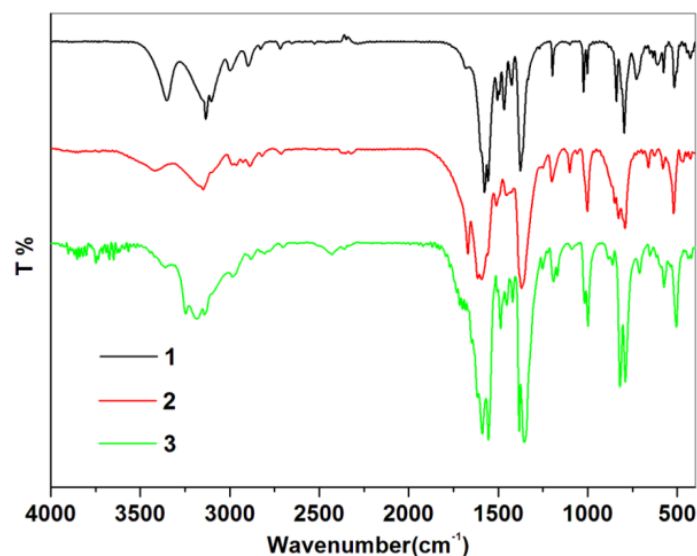


Fig. S11 IR spectra of **1-3**.

## 6. Oscilloscope traces of the SHG signals

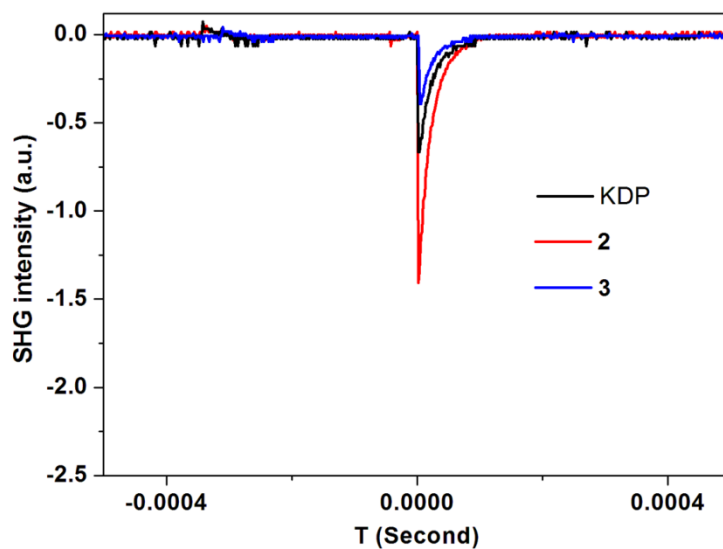
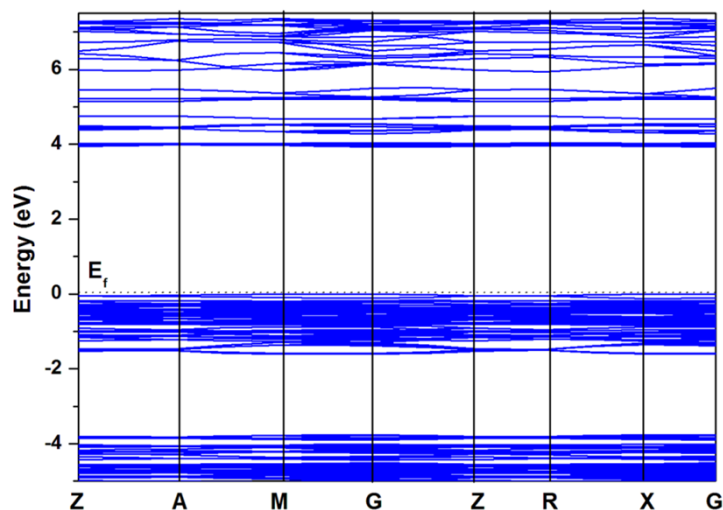
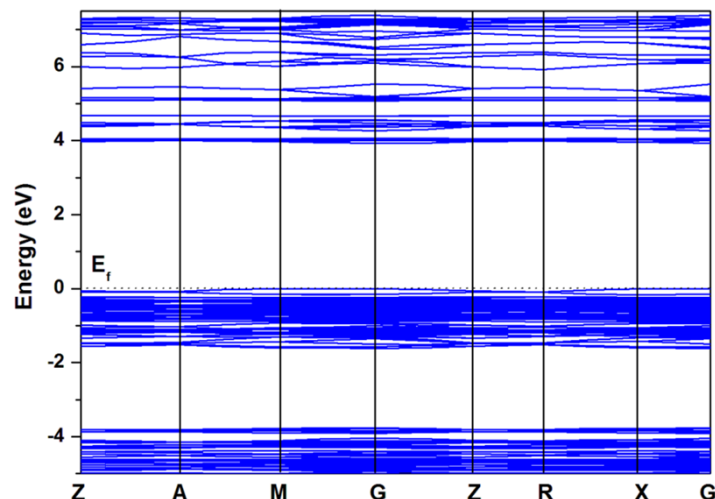


Fig. S12 Oscilloscope traces of the SHG signals of 2, 3 and KDP in the particle size of 150-212  $\mu\text{m}$ .

## 7. Theoretical calculation results

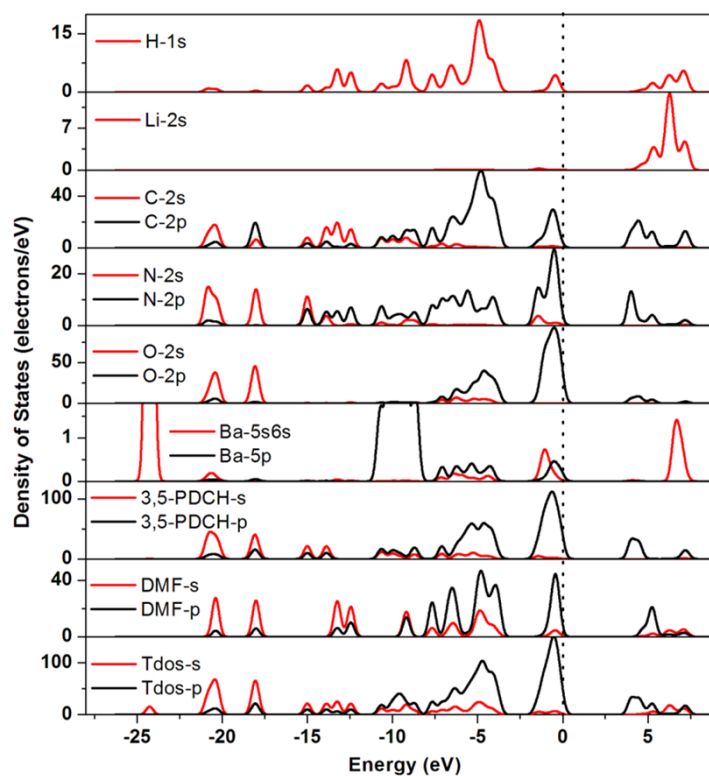
The density functional theory (DFT) studies were carried out for both **1** and **2** to study their energy band structures and optical properties. Since **1** and **2** are isostructural to each other, we take **1** as an example to analyse the calculated results. It can be seen from the band structures (Fig. S12) that both the highest occupied valence band (HVB) and the lowest unoccupied conduction band (LCB) are located at the G points. These features of the band structure indicate that **1** has flat valence band (VB), sparse conduction band (CB), and direct band gap.

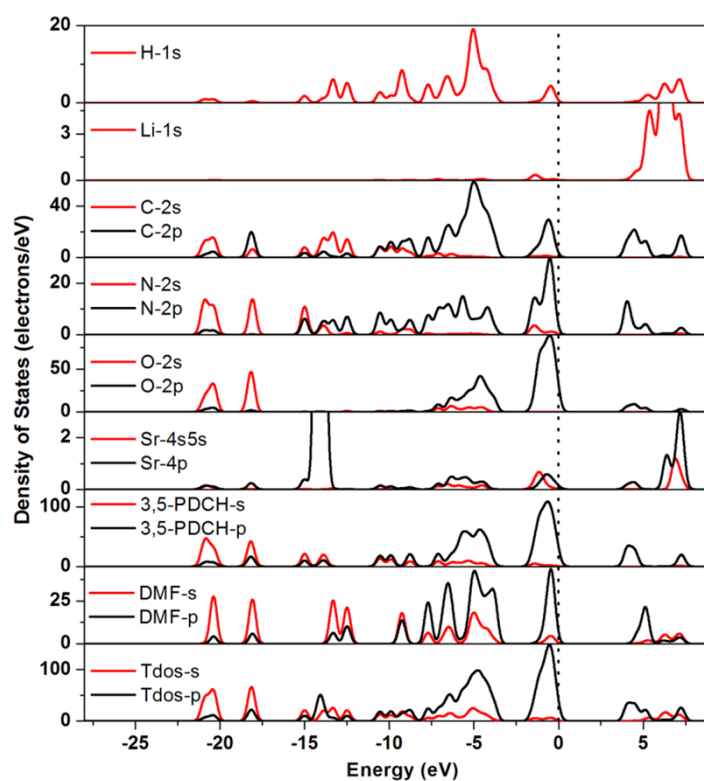




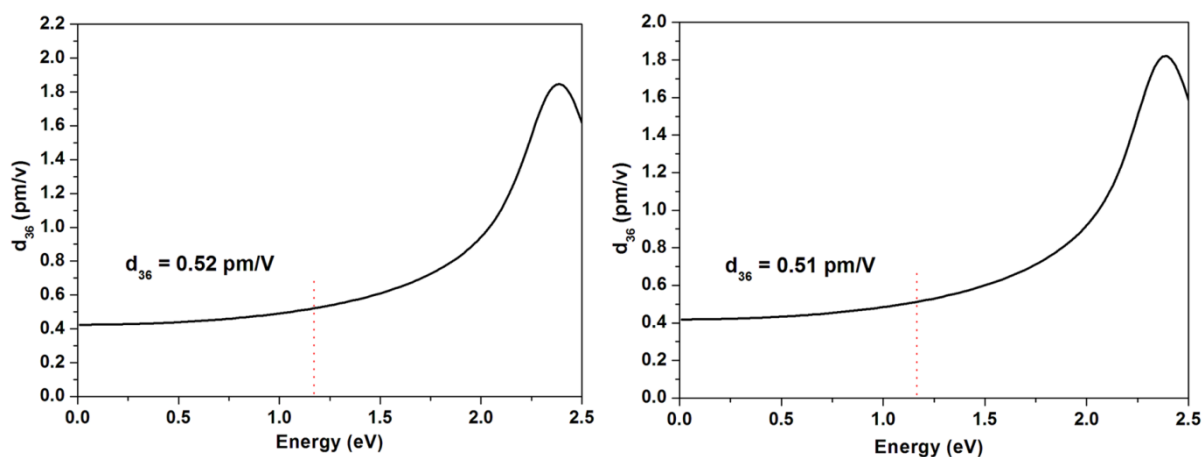
**Fig. S13** Electronic band structures for **1** (top) and **2** (bottom).

Figure S13 schematically illustrates the total density of states (TDOS) and partial density of states (PDOS) of **1** and **2**. With energy ranging from  $-8$  eV to the Fermi level, the VB region of **1** was dominated by the O-2p, N-2P, C-2P and H-1s states mixed with minor N-2s, C-2s, O-2s states and negligible Ba-5p6s and Li-2s states, whereas the CB (from 3 to 8 eV) is derived mainly from the C-2P, N-2P, O-2p states and a small mixture of Li-2s, H-1s, Ba-6s, C-2s, N-2s and O-2s states. Comparing the charge distributions nearby the Fermi level between the 3,5-PDCH<sup>2-</sup> ligand and DMF molecule, the contributions of the 3,5-PDCH-s and p states are more than that of DMF-s and p states in the VB region which is illustrated from the charge densities in the HVB region, Fig. 4. Moreover, the 3,5-PDCH-p state makes more contribution than the 3,5-PDCH-s state. Thus, it is obvious that the optical diffuse reflectance spectra is mainly ascribed to the charge transfers from the occupied 3,5-PDCH and DMF states to their unoccupied states and Ba-6s, Li-2s states.





**Fig. S14** Total and partial densities of states for **1** (top) and **2** (bottom). The Fermi level is set at 0 eV.



**Fig. S15** Calculated frequency-dependent second-harmonic generation tensor component  $d_{36}$  for **1** (left) and **2** (right). Frequency: 1064 nm (1.167 eV).

## 8. UV-vis diffuse reflectance spectra

The experimental band gap for compounds **1-3** are all 4.40 eV, Fig. S15.

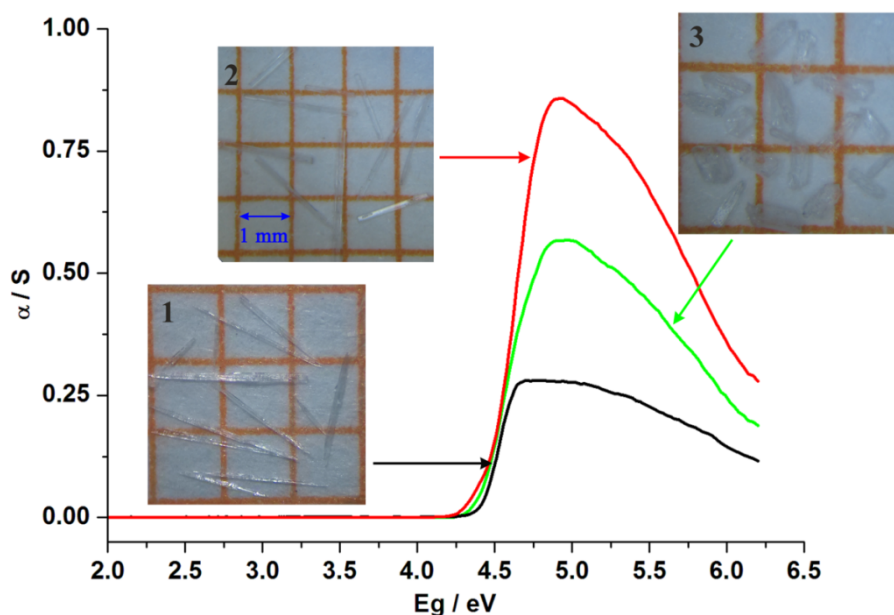


**Fig. S16** UV-vis diffuse reflectance spectra of **1-3**. Inserted are the crystal photographs of **1-3** under a microscopy.

## References:

- 1 S. K. Kurtz and T. T. Perry, *J. Appl. Phys.*, 1968, **39**, 3798-3813.
- 2 G. M. Sheldrick, *SHELX 97, Program for Crystal Structure Solution and Refinement*, University of Göttingen: Germany, 1997.
- 3 S. J. Clark, M. D. Segall, C. J. Pickard, P. J. Hasnip, M. J. Probert, K. Refson and M. C. Payne, *Z. Kristallogr.*, 2005, **220**, 567-570.
- 4 J. P. Perdew, K. Burke and M. Ernzerhof, *Phys. Rev. Lett.*, 1996, **77**, 3865-3868.
- 5 S. L. Dudarev, G. A. Botton, S. Y. Savrasov, C. J. Humphreys and A. P. Sutton, *Phys. Rev. B*, 1998, **57**, 1505-1509.
- 6 R. W. Boyd, *Nonlinear Optics*, Academic Press: New York, 1992, pp 21-47.
- 7 (a) D. Banerjee and J. B. Parise, *Cryst. Growth Des.*, 2011, **11**, 4704-4720; (b) T. Kundu, S. C. Sahoo and R. Banerjee, *Chem. Commun.*, 2012, **48**, 4998-5000; (c) L. Pan, T. Frydel, M. B. Sander, X. Y. Huang and J. Li, *Inorg. Chem.*, 2001, **40**, 1271-1283; (d) C. Pan, J. Nan, X. Dong, X.-M. Ren and W. Jin, *J. Am. Chem. Soc.*, 2011, **133**, 12330-12333.
- 8 (a) D. Banerjee, L. A. Borkowski, S. J. Kim and J. B. Parise, *Cryst. Growth Des.*, 2009, **9**, 4922-4926; (b) D. Banerjee, S. J. Kim, L. A. Borkowski, W. Q. Xu and J. B. Parise, *Cryst. Growth Des.*, 2010, **10**, 709-715; (c) M. K. Kim and K. M. Ok, *CrystEngComm*, 2011, **13**, 4599-4603.
- 9 (a) C. B. Liu, R. A. S. Ferreira, F. A. A. Paz, A. Cadiou, L. D. Carlos, L. S. Fu, J. Rocha and F. N. Shi, *Chem. Commun.*, 2012, **48**, 7964-7966; (b) P. King, R. Clerac, C. E. Anson and A. K. Powell, *Dalton Trans.*, 2004, 852-861.
- 10 J. S. Guo, G. Xu, X. M. Jiang, M. J. Zhang, B. W. Liu and G. C. Guo, *Inorg. Chem.*, 2014, **53**, 4278-4280.